Eco-Environment & Health 2 (2023) 107–116

Contents lists available at ScienceDirect

Eco-Environment & Health

journal homepage: www.journals.elsevier.com/eco-environment-and-health

Original Research Article

Alcohol consumption promotes arsenic absorption but reduces tissue arsenic accumulation in mice

Hongyu Wang [a], Albert L. Juhasz [b], Yaosheng Zhang [a], Lizhu Zhang [c], Lena Q. Ma [d], Dongmei Zhou [a], Hongbo Li [a,*]

[a] State Key Laboratory of Pollution Control and Resource Reuse, Jiangsu Key Laboratory of Vehicle Emissions Control, School of the Environment, Nanjing University, Nanjing 210023, China
[b] Future Industries Institute, University of South Australia, Mawson Lakes, South Australia 5095, Australia
[c] Department of Nanxin Pharm, Nanjing 210000, China
[d] Institute of Soil and Water Resources and Environmental Science, College of Environmental and Resource Sciences, Zhejiang University, Hangzhou 310058, China

ARTICLE INFO

Keywords:
Arsenic speciation
Alcohol consumption
Oral bioavailability
Tissue accumulation
Tight junctions

ABSTRACT

Alcohol consumption alters gut microflora and damages intestinal tight junction barriers, which may affect arsenic (As) oral bioavailability. In this study, mice were exposed to arsenate in the diet (6 μg/g) over a 3-week period and gavaged daily with Chinese liquor (0.05 or 0.10 mL per mouse per day). Following ingestion, 78.0% and 72.9% of the total As intake was absorbed and excreted via urine when co-exposed with liquor at daily doses of 0.05 or 0.10 mL, significantly greater than when As was supplied alone (44.7%). Alcohol co-exposure significantly altered gut microbiota but did not significantly alter As biotransformation in the intestinal tract or tissue. Significantly lower relative mRNA expression was observed for genes encoding for tight junctions in the ileum of liquor co-exposed mice, contributing to greater As bioavailability attributable to enhanced As absorption via the intestinal paracellular pathway. However, As concentration in the liver, kidney, and intestinal tissue of liquor-treated mice was decreased by 24.4%–42.6%, 27.5%–38.1%, and 28.1%–48.9% compared to control mice. This was likely due to greater renal glomerular filtration rate induced by alcohol, as suggested by significantly lower expression of genes encoding for renal tight junctions. In addition, in mice gavaged daily with 0.05 mL liquor, the serum antidiuretic hormone level was significantly lower than control mice (2.83 ± 0.59 vs. 5.40 ± 1.10 pg/mL), suggesting the diuretic function of alcohol consumption, which may facilitate As elimination via urine. These results highlight that alcohol consumption has a significant impact on the bioavailability and accumulation of As.

1. Introduction

Alcohol consumption is prevalent in vast populations [1,2]. Although many health effects of alcohol consumption or alcohol addiction, such as alcoholic liver, have been assessed [3–7], the impact on the absorption of a metal(loid) across the intestinal barrier, its entry into the bloodstream and organ sites (i.e., oral bioavailability), and its toxicity has rarely been investigated. Arsenic (As) is ubiquitous in the environment, and inorganic As (iAs) is classified as a class I human carcinogen [8–10]. Millions of people suffer from elevated As exposure via environmental exposure [11], including groundwater ingestion [12,13], consumption of food especially rice and rice-products [14], and incidental ingestion of As-contaminated soil and dust [15]. However, the subsequent health impacts are dose-dependent [15,16], which is influenced by bioavailability. Studies employing animal bioassays such as swine and mice have assessed As bioavailability in contaminated soil, dust, and food using urinary As excretion factor (the portion of the cumulative As intake recovered in the urine) as the bioavailability endpoint [17].

Since alcohol consumption is prevalent in adults and As is ubiquitous in the environment, their co-exposure may occur in the gastrointestinal (GI) tract. Alcohol co-exposure may affect As oral bioavailability via its role in altering the gut microbiota. Studies have shown that alcohol consumption may decrease the abundance of potentially beneficial genera, including *Bifidobacterium* and *Lactobacillus* and anti-inflammatory genera such as *Faecalibacterium*, and increase the abundance of Proteobacteria [18–20]. When iAs is ingested and passes

* Corresponding author.
E-mail address: hongboli@nju.edu.cn (H. Li).

https://doi.org/10.1016/j.eehl.2023.06.003
Received 30 March 2023; Received in revised form 11 June 2023; Accepted 25 June 2023
Available online 28 June 2023

through the GI tract, transformation of inorganic arsenate (iAs^V) to inorganic arsenite (iAs^{III}), monomethylarsonic acid (MMA^V), and dimethylarsinic acid (DMA^V) may occur via microbial transformation [21,22], although this may be influenced by processes such as alcohol consumption that affect gut microbiota composition [22–24]. This may influence As absorption as iAs^V and iAs^{III} are more readily absorbed than MMA^V and DMA^V [25,26].

Alcohol consumption may also affect As bioavailability via altering As transport across the intestinal barrier via transcellular and paracellular pathways. For transcellular transport, iAs^V may be absorbed via phosphate transporters such as type IIb sodium phosphate (*NaPi-IIb*) cotransporters in the apical membrane of intestinal enterocytes [27,28]. Paracellular As transport is strongly related to intestinal permeability, which is controlled by tight junctions located at the boundary between apical and basolateral membranes of enterocytes [29]. Animal (e.g., mice and rats) and human studies have shown that the alcohol use reduced mRNA and protein expression of intestinal tight junction proteins and increased intestinal paracellular permeability, causing "leaky gut" [19,30–32]. Following alcohol intake, the generation and accumulation of acetaldehyde in the intestine under the role of gut bacterial alcohol dehydrogenase can induce the inhibition and dissociation of intercellular protein tyrosine phosphatase-1B (PTP1B, a predominant role of dephosphorylation) from intercellular E-cadherin [33]. This process increases tyrosine phosphorylation of β-catenin and E-cadherin, which eventually damages paracellular tight junctions [33]. In addition, a high ethanol dose activates myosin light chain kinase (MLCK), increasing myosin II regulatory light chain phosphorylation and triggering perijunctional actomyosin ring contraction, eventually altering the cytoskeletal structure and thereby enhancing intestinal paracellular permeability [33–35]. With increased intestinal permeability, alcohol consumption may promote paracellular As transport, leading to greater As oral bioavailability and higher As accumulation in the body. However, alcohol consumption impacts dieresis, which is the body's defense mechanism to rapidly excrete absorbed alcohol and related metabolites via urine [36,37], which may promote As excretion via urine and lead to lower As retention in the body. Thus, the net effects of alcohol consumption on As accumulation in the body remain unclear.

The objective of this study was to assess alcohol effects on As oral bioavailability and As accumulation in tissue by conducting an *in vivo* mouse bioassay. Sodium arsenate was administered to mice via diet while mice were gavaged Chinese liquor. Underlying mechanisms were illustrated by assessing the effects on gut microbiota, As biotransformation, intestinal permeability, and renal permeability. It was hypothesized that alcohol co-exposure may alter As biotransformation, gut microbiota, and intestinal and renal permeability, affecting As oral bioavailability and As accumulation in tissue.

2. Materials and methods

2.1. Liquor and arsenic

Sodium hydrogen arsenate ($Na_2HAsO_4{\cdot}7H_2O$) was purchased from Sigma–Aldrich, while Beijing Erguotou Spirit (52° ethanol) was purchased from Trust-Mart Supermarket in Nanjing. It is a traditional Chinese Baijiu widely consumed by large Chinese populations. It was made from cooked sorghum, wheat, rice, and/or corn via fermentation under the role of alcohol yeast and collection of distillment when stewing. The predominant components of the liquor are alcohol (52%, v/v) and water. There are also some organic components such as advanced alcohols, methanol, polyols, aldehydes, carboxylic acids, and esters, but the total amount of these organic compounds is typically low (1%–2%) in the liquor. The concentrations of As, lead, and cadmium in the Baijiu were low (3.14 ± 0.51, 1.52 ± 1.19, and 0.02 ± 0.02 μg/L, $n = 10$), as suggested by determination using inductively coupled plasma mass spectrometry (ICP-MS, NexION300×, PerkinElmer, USA) after diluting 10 times using 0.1 M HNO_3. The Baijiu was selected rather than pure or industrial alcohol which is not consumed by humans, so the assessment of alcohol effects on As bioavailability using liquor is environmentally realistic.

2.2. Liquor dose determination

Before assessing the effects of alcohol co-exposure on As oral bioavailability and metabolism, the Beijing Erguotou Spirit was administered to adult mice [female, Balb/c, 6-week old, 20–22 g body weight (bw)] to determine a suitable dose to undertake co-exposure experiments. Mouse experiments were performed according to the Guiding Principles for Use of Animals of Nanjing University and approved by the Nanjing University Committee on Animal Care. Briefly, after acclimation under standard animal house conditions (12-h light/12-h dark cycle, 25 °C, and 50% humidity) for one week, 30 mice were divided into five groups (6 mice per group). Lee et al. [38] showed that the short-term (one week) low-dose [0.8 g/(kg bw·d)] consumption of ethanol significantly changed the gut microbiota composition in mice. Based on that, daily gavage of 0.02, 0.04, 0.10, and 0.20 mL of the Beijing Erguotou Spirit (52% ethanol) per mouse (20 g bw) was assessed, representing ethanol doses of 0.4–4.0 g/(kg bw·d). The daily administration of the Beijing Erguotou Spirit was kept for 3 weeks. At the end of the exposure period, liver samples were collected and separated into two with one sample stored in 10% paraformaldehyde solution prior to histopathology analysis and the other one immediately frozen in liquid nitrogen and stored at −80 °C prior to liver biochemical analyses.

2.3. Liquor and arsenic co-exposure in mice

After the observation that daily repeated gavage of ≤0.10 mL Beijing Erguotou Spirit per mouse did not cause obvious liver damage, the effect of Beijing Erguotou Spirit (0.05 and 0.10 mL per mouse per day) on As oral bioavailability was assessed. Briefly, after acclimation, 36 adult female mice (Balb/c, 6-week old, 20–22 g body weight) were randomly divided into six groups (six mice per group), i.e., mice with no As and no alcohol exposure ($^-As^-A$), mice with no As exposure but with daily gavage of 0.05 and 0.10 mL of Beijing Erguotou Spirit ($^-As^+A_{0.05}$ and $^-As^+A_{0.10}$), mice with As exposure but no alcohol exposure ($^+As^-A$), and mice with both As and alcohol exposure ($^+As^+A_{0.05}$ and $^+As^+A_{0.10}$).

For mice of $^-As^-A$, $^-As^+A_{0.05}$, and $^-As^+A_{0.10}$ groups, basal AIN-93G rodent diet was supplied for free consumption over three weeks, whereas sodium arsenate-amended AIN-93G diet (6 μg As/g) was supplied to mice in As exposure groups ($^+As^-A$, $^+As^+A_{0.05}$, and $^+As^+A_{0.10}$). An As concentration of 6 μg As/g was based on the reports of As concentration in food such as rice up to ~2 μg/g [39] and gut microbiome disruption studies that utilized a drinking water concentration of 10 μg As/mL [40,41]. During the 3-week period, each mouse in the alcohol exposure groups received a gavage of Beijing Erguotou Spirit (0.05 or 0.10 mL) daily and free consumption of corresponding diets. Mice were housed in polyethylene cages on dry wood chip bedding with two mice per cage over the initial two weeks. The difference in total diet supplied and those remaining at the end of the 2-week exposure was recorded as diet consumption amount. Subsequently, mice were transferred into metabolic cages (two mice in a cage) for the remaining 7 d to collect urine and feces samples. For the 7-d exposure period using metabolic cages, diet was also freely consumed with the diet consumption amount also recorded. The product of diet As concentration and total diet consumption was used to determine cumulative As intake.

Urine and feces were collected daily from metabolic cages in the last week of exposure. At the end of the exposure, urine and feces samples from two mice in a cage over the 7-d period were pooled to get cumulative urine and feces samples. The body weight of mice was recorded and blood was collected into coagulation tubes and then centrifuged (3,500 rpm, 10 min) to obtain serum prior to storage at −80 °C. The kidneys of each mouse were collected separately, with one used for As accumulation and speciation analysis and the other used for biochemical and renal tubule tight junction protein gene expression analyses. Livers

were also collected and divided into two subsamples with one used for As accumulation and speciation analysis and the other used for biochemical analyses. The intestinal tract from duodenum to cecum was dissected, with luminal contents collected for gut microbiota analyses. From the middle part of the ileum, a section of about 0.5 cm was dissected and stored in 10% paraformaldehyde solution for histopathology analysis, while the remaining ileum was immediately frozen in liquid nitrogen and stored at −80 °C for tight junction protein gene expression and PTP1B and MLCK analysis. The remaining intestinal tract tissue was collected as a combined sample for As accumulation and speciation analysis.

2.4. Determination of As concentration and As bioavailability

Mouse feces and tissue (e.g., intestinal tract tissue, liver, and kidney) samples were freeze-dried (Freezone Plus 6, Labconco, USA), ground to powders, and digested subsequently using diluted HNO_3 (v/v = 1:1) and H_2O_2 (30%) (USEPA Method 3050 B) prior to analysis of As concentration by ICP-MS. Urine samples were centrifuged (3,000 rpm, 10 min), filtered (0.45 μm), and diluted using 0.1 mM HNO_3 prior to analysis using ICP-MS.

Prior to its excretion via urine, As is absorbed across the intestinal barrier to blood and transported to kidney. Studies have shown that the predominant proportion of the absorbed As is readily excreted via urine, while <1% of absorbed As ends in tissue such as liver and kidneys [17,21,22]. So, analyses of the amount of As excreted in urine is a predominant and sensitive endpoint for assessing As oral bioavailability. As urinary excretion factor (UEF, %) was calculated to determine As oral bioavailability (Eq. 1).

$$\text{As UEF}\ (\%) = \frac{U_{\text{As}} \times V_{\text{urine}}}{D_{\text{As}} \times W} \times 100\% \quad (1)$$

where, U_{As} is the As concentration in cumulative urine samples (μg As/mL) excreted by mice in the last week of exposure, V_{urine} is the volume of cumulative urine samples (mL), D_{As} is the As concentration in diet (6 μg As/g), and W is the weight of diet consumption of mice in the last week of exposure (g).

2.5. Arsenic speciation

Mouse intestinal tract tissue, intestinal contents, liver, kidney, and feces samples from $^{+}As^{-}A$, $^{+}As^{+}A_{0.05}$, and $^{+}As^{+}A_{0.10}$ groups were extracted twice using a methanol/Milli-Q water (1:1 v/v, 2 mL) solution for 2 h in an ultrasonic ice water bath. Extracts were combined, filtered through 0.2 μm filters, and stored at −80 °C prior to analysis. Urine samples were diluted 200 times with Milli-Q water. High performance liquid chromatography (HPLC, Waters e2695, USA) coupled with ICP-MS and equipped with an anion-exchange column (PRP-X100, 4.1 × 250 mm, 10 μm, Hamilton, UK) and a guard column (Hamilton, UK) was used to separate and identify six As species including iAs^{III}, DMA^{V}, MMA^{V}, $DMMTA^{V}$, $MMMTA^{V}$, and iAs^{V}. The mobile phase consisted of 3.5 mM NH_4HCO_3 and 5% methanol at pH 8.5 with a flow rate of 1.0 mL/min. By comparing the sum of six As species by HPLC-ICP-MS to As concentration by ICP-MS, the As recovery rates ranged from 55% to 80%.

2.6. Liver and ileum histopathology

Liver samples from liquor dose determination experiments and ileum sections from liquor and As co-exposure experiments (fixed in 10% paraformaldehyde solution) were embedded in paraffin, sliced to 5 μm thickness with a microtome (Leica RM2016, Germany), followed by dehydration and conventional hematoxylin-eosin (H&E) staining and photography under a light microscope (Nikon Eclipse CI, Japan) [19]. Liver cell shrinkage and structure and defective intestinal tight junction barriers were assessed.

2.7. Serum, liver, kidney, and ileum biochemical analysis

Liver samples from liquor dose determination experiments and serum samples from liquor and As co-exposure experiments were assessed for malondialdehyde (MDA) concentration and superoxide dismutase (SOD) and glutathione peroxidase (GSH-px) activities using mouse ELISA Kits (CB10305-Mu, CB10324-Mu, and CB10476-Mu, Shanghai Keaibo Biotechnology Co., Ltd, China). Metallothionine (MT) concentration in the liver and kidneys of As exposed mice were measured using a mouse ELISA Kit (CB10619-Mu, Shanghai Keaibo Bio-technology Co., Ltd, China) on a Thermo Scientific Microplate Reader (Multiskan FC). The activities of PTP1B and MLCK in the ileum of As exposed mice were measured using mouse ELISA Kits (MM-1160M1 and MM-46939M1, Jiangsu Meimian Industrial Co., Ltd, China). Serum levels of antidiuretic hormone (ADH) were measured using a mouse ELISA Kit (CB10661-Mu, Shanghai Keaibo Bio-technology Co., Ltd, China).

2.8. Gut microbiota characterization

Thirty-six intestinal content samples from $^{-}As^{-}A$, $^{-}As^{+}A_{0.05}$, $^{-}As^{+}A_{0.10}$, $^{+}As^{-}A$, $^{+}As^{+}A_{0.05}$, and $^{+}As^{+}A_{0.10}$ groups were characterized for gut microflora. For each treatment, two intestinal content samples from the two mice moused in a husbandry cage were combined and thoroughly mixed using RNA-free water. Stool Genomic DNA kits (Win Biotech Co., Ltd, Beijing, China) were used to extract genomic DNA from eighteen combined intestinal samples (n = 3 for each treatment). Genomic DNA was amplified using polymerase chain reaction (PCR) (GeneAmp® 9700, ABI, USA) targeting bacterial V3–V4 regions of the 16s rRNA gene. A NanoDrop ND-1000 spectrophotometer (Thermo Fisher Scientific, USA) was used to quantify PCR products, while individual samples were sequenced using an Illumina Novaseq 6000 platform (Genepioneer Biotechnologies, Nanjing, China). Original sequence data were deposited in NCBI SRA (the accession number: PRJNA932253). The details on sequence data processing are provided in the Supporting Information (SI).

2.9. RNA isolation and quantitative real time PCR

The effect of liquor co-exposure on gene expression of ileum tight junctions [*Zona-Occludins 1* (*ZO-1*), *Cingulin*, and *Fodrin/Spectrin alpha*] and phosphate transporter (*NaPi-IIb*) that are involved in paracellular and transcellular iAs^{V} transport were assessed. In addition, the effect of liquor co-exposure on gene expression of renal tight junctions (*ZO-1, Cingulin, Fodrin/S. alpha*, *Claudin 1*, *Claudin 4*, *Occludin*, and *Symplekin*) which controls paracellular permeability across the glomerular barrier was also determined.

Total RNA was extracted and purified from fresh ileum sections (~0.5 cm length) and kidney sections (~10 mg) using the FastPure Cell/Tissue Total RNA Isolation Kit V2 (Nanjing Vazyme Biotech Co., Ltd., China) as per manufacturer's instructions. RNA concentration and purity were measured using a NanoDrop One spectrophotometer (Thermo Fisher Scientific, USA). Reverse transcription of RNA (1 μg) to cDNA was conducted using HiScript III RT SuperMix for qPCR (+gDNA wiper) Kit (Nanjing Vazyme Biotech Co., Ltd., China). Real time quantitative PCR was performed using Hieff UNICON qPCR SYBR Green Master Mix (CAT: 11198ES08, Yeasen Biotech CO., Ltd., China) on a Bio-Rad Real-Time PCR System (T100™ Thermal Cycler). Gene-specific primers are shown in Table S1. mRNA expression data are expressed using the $2^{-\Delta\Delta C}$ method [42].

2.10. Quality assurance/quality control and data processing

The mean and standard deviation of replicate analyses (n = 3 or 6) were used to present all data. At least three blanks were included during each digestion batch. Triplicate measurements were conducted for each sample during analysis using ICP-MS, with a relative standard deviation

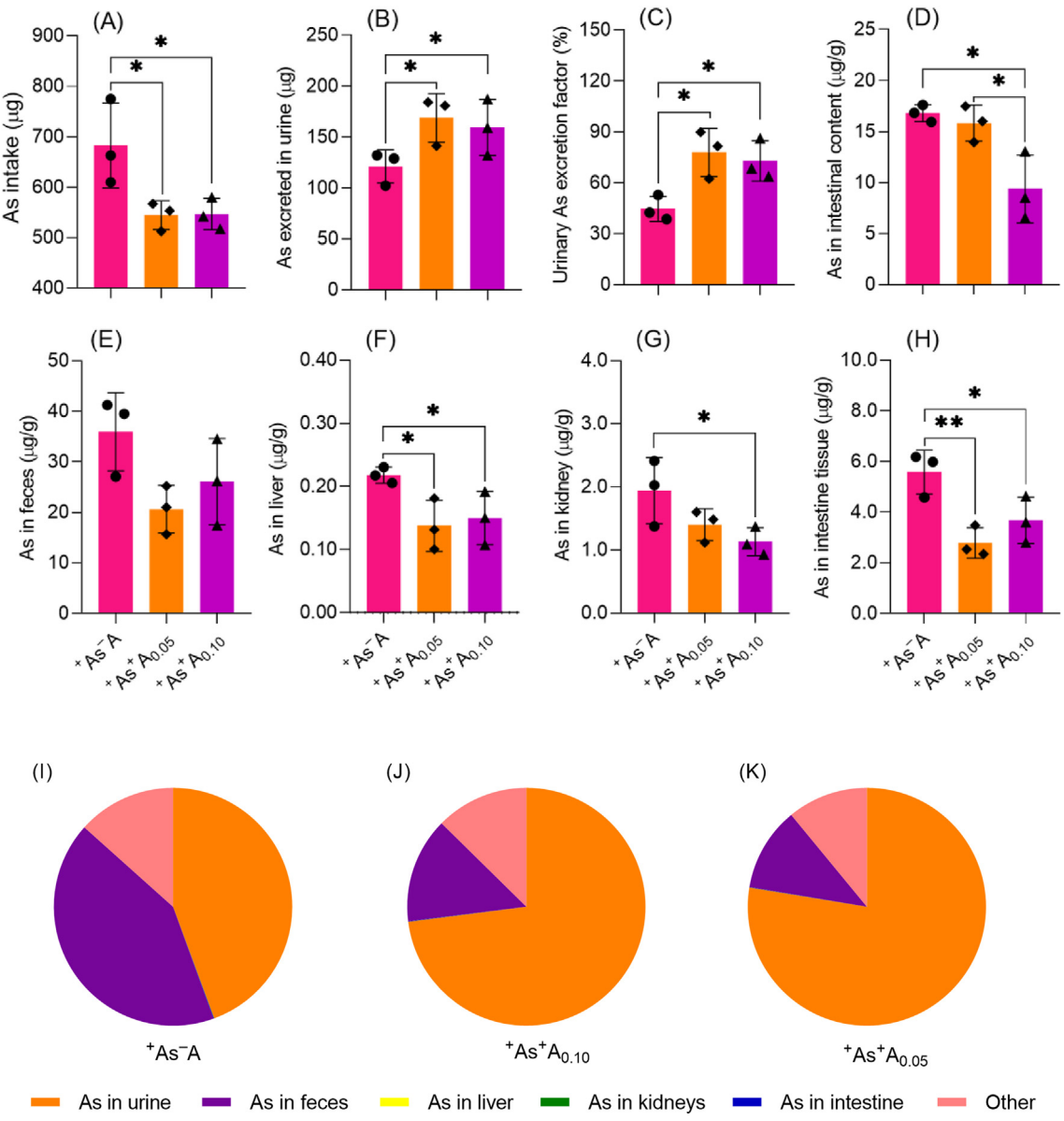

Fig. 1. Effects of alcohol consumption on cumulative As intake via diet over a 3-week period (**A**), cumulative As excreted in urine during the 3rd week of exposure (**B**), urinary As excretion factor during the 3rd week of exposure (**C**), As concentration in intestinal luminal contents (**D**), feces (**E**), liver (**F**), kidney (**G**), and intestine tissue (**H**) after the 3-week period for mice fed with diets containing 6 μg As/g. Mass balance calculation showing recovery of As intake in As in mouse urine, feces, liver, kidneys, intestine, and As retention in other organs (**I–K**). $^{+}As^{-}A$ represents mice fed with diet containing As without alcohol co-exposure; $^{+}As^{+}A_{0.05}$ and $^{+}As^{+}A_{0.10}$ represent mice fed with diets amended with As and daily gavaged with 0.05 and 0.10 mL Chinese liquor (52° ethanol Beijing Erguotou Spirits) per mouse over a 3-week period. * and **, significant difference at $p < 0.05$ and 0.01, respectively.

being <0.5%. Standard solutions were measured using ICP-MS with every 20 samples, with the recoveries of 95%–105% (n = 10). An indium isotope (^{114}In) was used as an internal standard to monitor the stability of ICP-MS analyses, with ^{114}In recoveries being 95%–105%. Student's t-test was conducted to assess significant differences between different groups using IBM SPSS Statistics at $\alpha = 0.05$.

3. Results and discussion

3.1. Liquor dose determination

After 3-week daily gavage of 0.10–0.20 mL of Beijing Erguotou Spirit per mouse, mouse liver GSH-px and SOD levels were 22%–36% and 28%–30% lower ($p < 0.05$) than the control mice that did not receive liquor. When doses were lower (0.02 and 0.04 mL per mouse per day), a decrease in GSH-px and SOD was also observed (by 9%–19% and 10%–12% compared to control mice, respectively), although the differences were insignificant ($p > 0.05$) (Fig. S1A, B). Liquor consumption led to higher liver MDA levels (Fig. S1C), suggesting oxidative stress in the liver. Liquor doses at 0.02–0.10 mL per mouse per day did not cause obvious liver histopathological changes compared to control mice, whereas a dose of 0.20 mL led to significant liver cell shrinkage and irregular structure (Fig. S2). These results suggest that the mouse antioxidant system may not overcome oxidative stress derived from liquor doses >0.10 mL per mouse per day. Hence, daily liquor doses of 0.05 mL and 0.10 mL per mouse per day were selected to assess alcohol effects on As oral bioavailability thereafter.

3.2. As bioavailability and retention in the body

During the 3-week liquor and As co-exposure studies, $^{+}As^{+}A_{0.05}$ and $^{+}As^{+}A_{0.10}$ mice showed significantly ($p < 0.05$) lower total diet

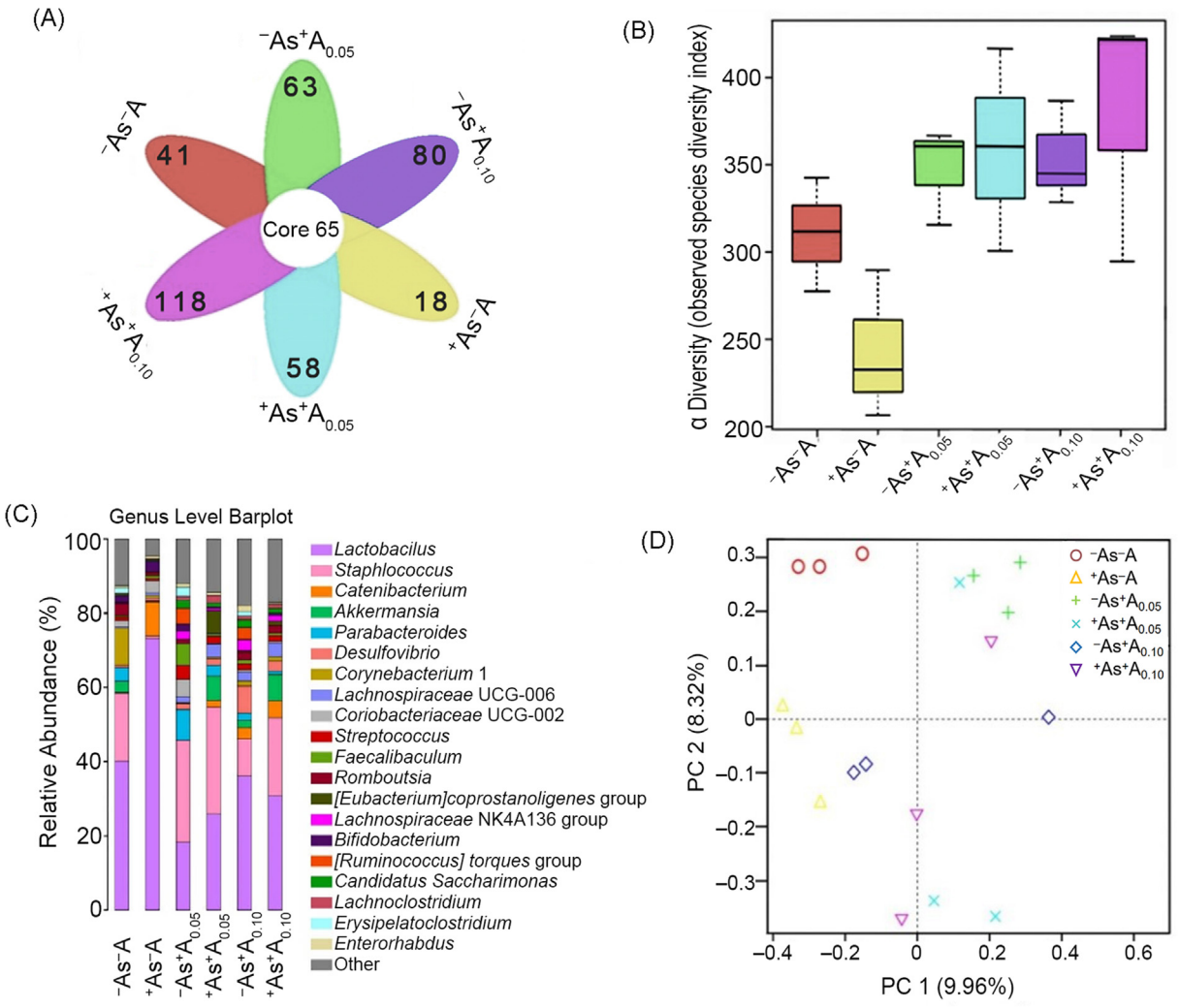

Fig. 2. Variation in the composition of mouse gut microbiota among non-As and As exposed mice without and with alcohol co-exposure. (**A**) The petal plot shows the number of shared OTUs as well as the number of unique OTUs among mice with no As and no alcohol exposure ($^{-}As^{-}A$), mice with no As but with daily repeated gavage of 0.05 and 0.10 mL of Beijing Erguotou Spirit ($^{-}As^{+}A_{0.05}$, $^{-}As^{+}A_{0.10}$), mice with As exposure but no alcohol exposure ($^{+}As^{-}A$), and mice with both As and alcohol exposure ($^{+}As^{+}A_{0.05}$, $^{+}As^{+}A_{0.10}$). (**B**) Boxplot of α diversity of mouse gut bacterial communities of different treatment groups. (**C**) Composition of mouse gut microbiota at the genus level. Genera showing levels with <1% of total number of reads were categorized as "Other." (**D**) Principal coordinates analysis revealing the distribution of mouse gut bacterial communities according to OTU based on Bray_Curtis distance.

consumption (90.8 ± 4.75 and 91.2 ± 5.22 vs. 114 ± 14.1 g) than mice exposed to $^{+}As^{-}A$ mice, which led to a significantly ($p < 0.05$) lower cumulative As intake in the alcohol-treated mice (544 ± 28.5 and 545 ± 31.3 vs. 683 ± 84.4 μg As) (Fig. 1A). However, during the 3rd week of exposure, significantly ($p < 0.05$) higher amounts of As were excreted in the urine of $^{+}As^{+}A_{0.05}$ and $^{+}As^{+}A_{0.10}$ mice than $^{+}As^{-}A$ mice (169 ± 23.8 and 160 ± 27.6 vs. 121 ± 16.3 μg As) (Fig. 1B). By calculating As UEF (Eq. 1), As bioavailability was 78.0% ± 14.1% and 72.9% ± 11.9% in $^{+}As^{+}A_{0.05}$ and $^{+}As^{+}A_{0.10}$ mice, significantly ($p < 0.05$) higher than that of $^{+}As^{-}A$ mice (44.7% ± 7.36%) (Fig. 1C). The UEF of $^{+}As^{-}A$ mice was slightly lower than previous reports of 57.8% ± 4.8% to 63.0% ± 7.2% [15]. Compared to $^{+}As^{-}A$ mice (16.8 ± 0.84 μg/g), significantly ($p < 0.05$) lower As concentrations were observed in the intestinal tract contents of $^{+}As^{+}A_{0.10}$ mice (9.39 ± 3.33 μg/g), while As concentrations in feces of $^{+}As^{+}A_{0.05}$ and $^{+}As^{+}A_{0.10}$ mice (20.7 ± 4.78 and 20.1 ± 8.53 μg/g) were lower than $^{+}As^{-}A$ mice (31.0 ± 7.72 μg/g) (Fig. 1D and E). These results suggest that the ingested iAs^{V} was more readily absorbed with liquor co-exposure, with about 80% of As intake being absorbed and excreted via urine, leading to less non-bioavailable As remaining in feces.

For $^{+}As^{+}A_{0.05}$ and $^{+}As^{+}A_{0.10}$ mice, As concentrations in the liver, kidney, and the intestinal tract tissue were 0.14–0.15, 1.13–1.40, and 2.80–3.69 μg/g, significantly lower ($p < 0.01$) than those of $^{+}As^{-}A$ mice (0.22 ± 0.01, 1.94 ± 0.52, and 5.59 ± 0.87 μg/g) (Fig. 1F–H). These data indicate that although liquor co-exposure increased As oral bioavailability, greater As absorption from the GI tract did not translate into greater As accumulation in tissue.

Mass balance calculation showed that in $^{+}As^{-}A$ mice, 44.7% and 42.1% of total As intake was recovered in urine and feces, while As accumulation in the liver, kidney, and intestine contributed only 0.01%–0.08% (Fig. 1I). In comparison, in $^{+}As^{+}A_{0.05}$ and $^{+}As^{+}A_{0.10}$ mice, the recovery of As in urine was elevated to 72.9%–78.0% while that of As in feces was reduced to 11.4%–14.3% (Fig. 1J and K), confirming that As bioavailability was increased with liquor consumption.

3.3. Gut microbiota

Alcohol consumption can cause an overgrowth of gut microbiota and re-shape the gut microbial community, causing an imbalance of gut bacteria [24,43], which may influence As metabolism and bioavailability

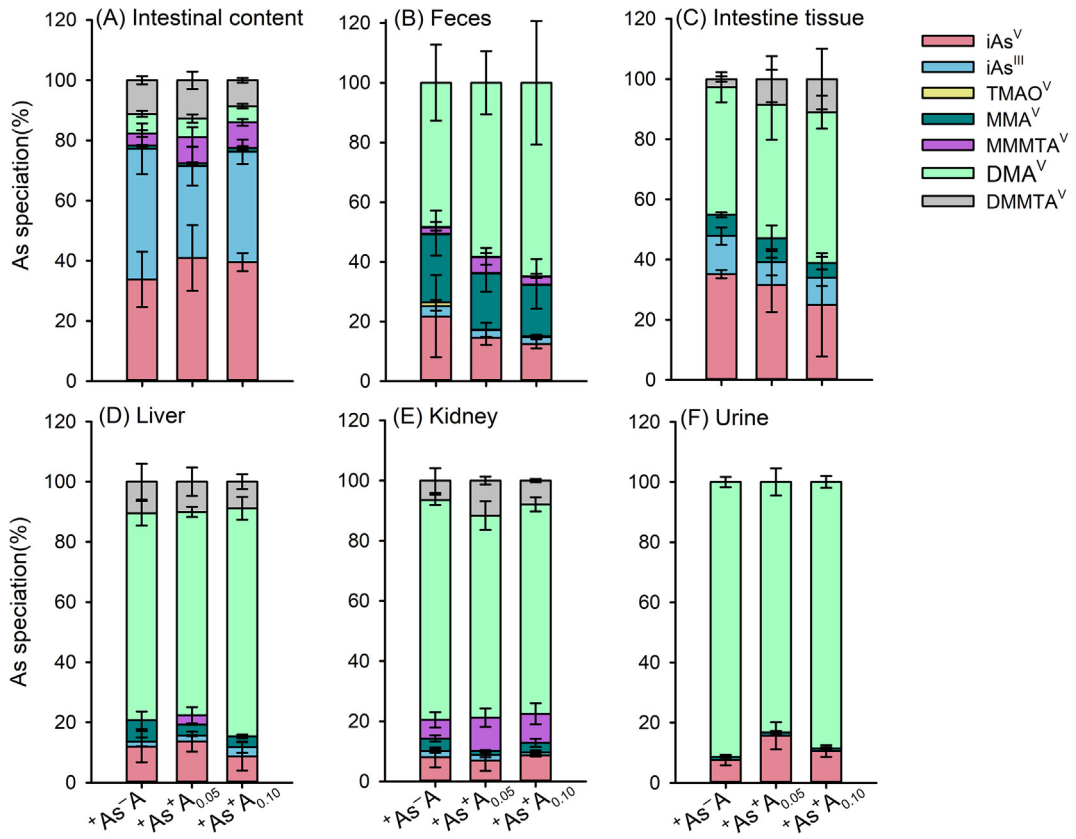

Fig. 3. Effect of alcohol consumption on As speciation in intestinal tract contents (**A**), feces (**B**), intestine tissue (**C**), liver (**D**), kidney (**E**), and urine (**F**) of mice fed with diets containing 6 μg As/g.

[44]. To explain the higher As oral bioavailability in the presence of alcohol, the composition of gut microbiota was determined for control and exposed mice.

The alteration of mouse gut microbial diversity and community compositions with As exposure has been investigated [40]. In this study, $^{+}$As^{-}A mice showed lower gut microbial diversity than $^{-}$As^{-}A mice, as suggested by a lower number of OTUs (Operational Taxonomic Units) unique to $^{+}$As^{-}A mice than those unique to $^{-}$As^{-}A mice (18 vs. 41) (Fig. 2A). In addition, compared to $^{-}$As^{-}A mice, the observed species diversity index was significantly lower in $^{+}$As^{-}A mice (Fig. 2B), confirming that As exposure lowered gut bacterial diversity. In addition, there were significant differences in gut microbial community compositions between $^{+}$As^{-}A and $^{-}$As^{-}A mice. Compared to $^{-}$As^{-}A mice, As exposure in $^{+}$As^{-}A mice increased relative abundance of *Lactobacillus* (73.2% vs. 40.2%) and *Catenibacterium* (9.23% vs. 0.20%), while growth of *Staphlococcus* (0.73% vs. 18.3%), *Akkermansia* (0.002% vs. 3.01%), *Parabacteroides* (0.22% vs. 3.67%), and *Corynebacterium* (0.64% vs. 10.0%) was significantly inhibited (Fig. 2C). Principal coordinates analysis (PCoA) according to OTU based on Bray_Curtis distance showed separation between $^{+}$As^{-}A and $^{-}$As^{-}A mice (Fig. 2D), indicating As exposure reshaped the gut microbial community in this study.

Regardless of the presence or absence of As, liquor consumption significantly influenced the composition of gut microbiota, stimulating the growth of many minor bacteria, leading to higher bacterial diversity. This was reflected by higher numbers of OTUs unique to $^{-}$As^{+}A$_{0.05}$ and $^{-}$As^{+}A$_{0.10}$ mice (63 and 80) and $^{+}$As^{+}A$_{0.05}$ and $^{+}$As^{+}A$_{0.10}$ mice (58 and 118) compared to $^{-}$As^{-}A and $^{+}$As^{-}A mice (41 and 18) (Fig. 2A). Also, compared to $^{-}$As^{-}A and $^{+}$As^{-}A mice, the four groups of liquor-treated mice showed significantly ($p < 0.05$) greater variability in species diversity, demonstrating higher α diversity (Fig. 2B). The higher species diversity caused by liquor treatment may be due to the enrichment of many minor bacteria after alcohol ingestion. As a readily available carbon and energy source, ethanol in the intestine can be used as a growth substrate and stimulate the growth of gut bacteria that is initially low in abundance [18–20].

At the genus level, $^{+}$As^{+}A$_{0.05}$ and $^{+}$As^{+}A$_{0.10}$ mice showed significantly ($p < 0.05$) lower relative abundance of *Lactobacillus* (25.9%–30.9% vs. 73.2%) and *Catenibacterium* (1.74%–4.59% vs. 9.23%) than $^{+}$As^{-}A mice (Fig. 2C). In comparison, many bacteria such as *Staphlococcus*, *Akkermansia*, *Parabacteroides*, *Desulfovibrio*, and *Lachnospiraceae* UCG-006 that were detected in $^{+}$As^{-}A mice at low abundances (0.73%, 0.002%, 0.22%, 0.81%, and 0.71%) were significantly ($p < 0.05$) enriched in the gut of $^{+}$As^{+}A$_{0.05}$ and $^{+}$As^{+}A$_{0.10}$ mice (20.9%–28.8%, 6.67%–7.13%, 0.90%–2.82%, 1.75%–2.68%, and 3.55%–3.79%). A decrease in potentially beneficial bacteria *Lactobacillus* and an increase in the proportion of *Proteus*, *Fusobacteria*, *Enterobacteriaceae*, and *Halomonadaceae* have been reported in alcoholic humans [32,45]. PCoA based on Bray_Curtis distance showed separation between $^{+}$As^{-}A mice with $^{+}$As^{+}A$_{0.05}$ and $^{+}$As^{+}A$_{0.10}$ mice and between $^{-}$As^{-}A mice with $^{-}$As^{+}A$_{0.05}$ and $^{-}$As^{+}A$_{0.10}$ mice (Fig. 2D), confirming that liquor co-exposure significantly altered gut microbial community composition.

3.4. As metabolism in the GI tract and post-absorption

Gut microbiomes participate in As biotransformation in the GI tract, converting iAs^{V} to iAs^{III}, MMA^{V}, and DMA^{V} [23,24]. In the intestinal tract contents of As-treated mice, ~60% of iAs^{V} was transformed to other species, as shown by iAs^{V}, iAs^{III}, MMA^{V}, MMMTA^{V}, DMA^{V}, and DMMTA^{V} contribution of 33.8%–40.9%, 30.5%–43.5%, 0.95%–1.25%, 4.00%–8.68%, 5.41%–6.53%, and 8.60%–12.80% to total As concentration (Fig. 3A). In feces, DMA^{V} became the predominant As species (48.5%–65.0%), followed by MMA^{V} (17.2%–22.8%), whereas iAs^{V}, iAs^{III}, MMMTA^{V}, and

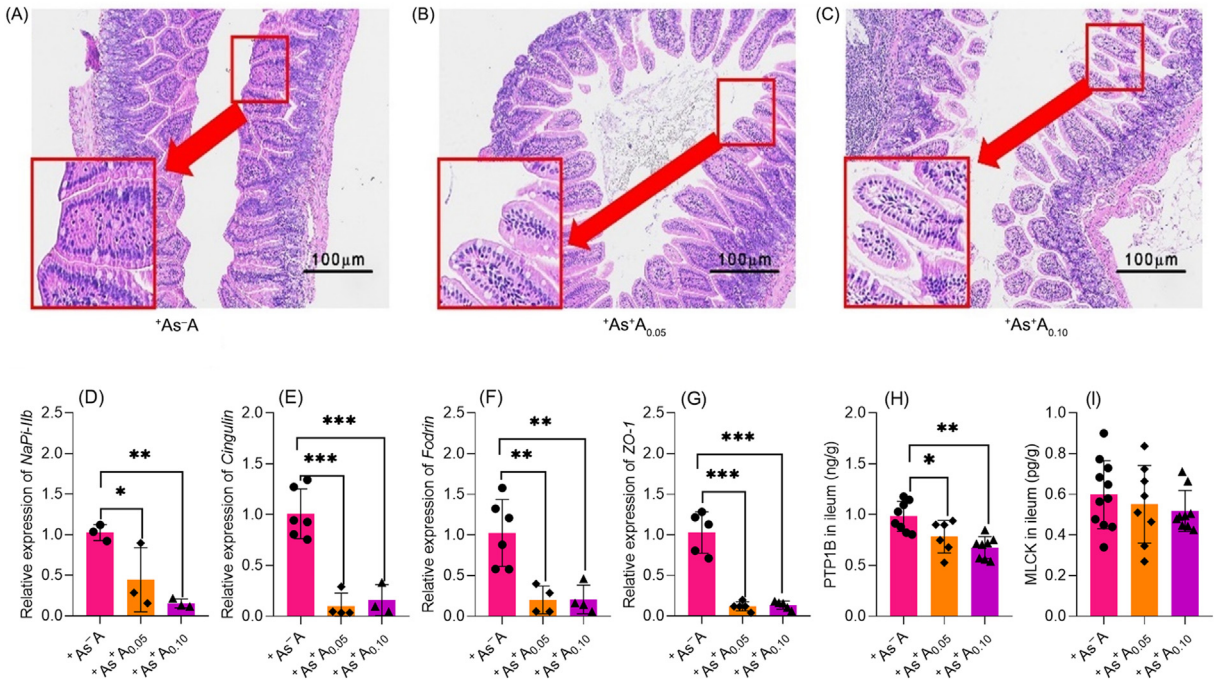

Fig. 4. Hematoxylin-eosin (H&E) staining showing ileum morphologies of mice fed with diets amended with As (6 μg As/g) without and with alcohol co-exposure (**A–C**). Comparison of the ileum relative expression of *NaPi-IIb* in alcohol-treated mice to As exposed control mice (**D**). Comparison of the relative expression of genes encoding for tight junctions (TJs) in the ileum including *Cingulin* (**E**), *Fodrin* (**F**), and *Zona-Occludins 1* (*ZO-1*, **G**) between alcohol-treated and As exposed control mice. Comparison of PTP1B (**H**) and MLCK (**I**) levels in the ileum between alcohol-treated and As exposed control mice. ***, significant difference at $p < 0.001$.PTP1B, protein tyrosine phosphatase-1B. MLCK, myosin light chain kinase.

$DMMTA^V$ contribution sharply decreased to 12.4%–21.6%, 2.36%–3.57%, 2.27%–5.36%, and 0.23%–1.25% (Fig. 3B). Passing through the GI tract, iAs^V and iAs^{III} were more readily absorbed into the blood than MMA^V and DMA^V [22,23], which in turn may cause a decrease in iAs^V and iAs^{III} and an increase in the percent contribution of MMA^V and DMA^V in feces.

Following absorption, the transformation of highly toxic inorganic As to less toxic DMA^V in tissue is an important As detoxification mechanism for mammals [46,47]. In this study, As biotransformation after absorption was observed, with DMA^V becoming the predominant As species. In small intestinal tract tissue of $^{+}As^{-}A$, $^{+}As^{+}A_{0.05}$, and $^{+}As^{+}A_{0.10}$ mice, 24.9%–35.1%, 7.55%–12.7%, 4.84%–7.95%, 42.4%–50.2%, and 2.71%–11.03% of total As was iAs^V, iAs^{III}, MMA^V, DMA^V, and $DMMTA^V$, respectively (Fig. 3C). In the liver and kidney, DMA^V contribution was 67.6%–75.8% and 67.1%–73.1%, respectively (Fig. 3D and E). In urine, DMA^V contribution was 83.3%–91.2%, with 7.60%–15.6% of total As being present as iAs^V (Fig. 3F). Our previous study showed similar results that DMA^V became the predominant As species present in liver, kidney, and urine of mice exposed to iAs^V [22].

Arsenic speciation biotransformation in the GI tract may be involved by gut microbiota [44]. However, while gut microbiota differed significantly between $^{+}As^{+}A_{0.05}$, $^{+}As^{+}A_{0.10}$, and $^{+}As^{-}A$ mice (Fig. 2), their ability to metabolize inorganic As to methylated As in the GI tract may not be significantly affected by liquor consumption, as suggested by similar As speciation in the intestinal tract contents of these mice (Fig. 3A). In addition, As speciation in the small intestinal tract tissue, liver, kidney, and urine of liquor-treated mice was similar to As control mice, although some minor but insignificant ($p > 0.05$) differences were observed. Our previous study showed that although adult and weanling mice differed significantly in the composition of mouse gut microbiota, their As biotransformation in the GI tract, blood, liver, kidney, and urine was similar [22]. Thereby, gut microbiota and As biotransformation alterations may not be important factors influencing higher As oral bioavailability and lower As tissue accumulation in liquor-treated mice.

3.5. Intestinal and renal permeability

Compared to As exposed control mice, a relative expression of *NaPi-IIb* in the ileum of liquor-treated mice was significantly reduced (Fig. 4D), suggesting possible down-regulation of phosphate transporter expression involved in iAs^V transcellular transport. These results were contrary to the significantly higher As bioavailability in liquor-treated mice (Fig. 1C), suggesting that altered iAs^V transcellular transport via phosphate transporters was not a mechanism contributing to elevated As bioavailability.

Defective intestinal tight junction barriers were observed in mice with liquor co-exposure, which may be an important contributor to greater As bioavailability. H&E staining of ileum sections showed that enterocytes of $^{+}As^{-}A$ mice were tightly connected with each other (Fig. 4A), whereas liquor co-exposure caused loosened connections between intestinal enterocytes of $^{+}As^{+}A_{0.05}$ and $^{+}As^{+}A_{0.10}$ mice, suggesting damaged tight junctions (Fig. 4B and C). This was also evidenced by significantly ($p < 0.05$) lower relative mRNA expression of genes encoding for tight junction proteins including *Cingulin* (0.10 ± 0.13 and 0.16 ± 0.15 vs. 1.00 ± 0.24), *Fodrin* (0.20 ± 0.17 and 0.21 ± 0.18 vs. 1.02 ± 0.41), and *ZO-1* (0.12 ± 0.05 and 0.15 ± 0.05 vs. 1.03 ± 0.25) in the ileum of $^{+}As^{+}A_{0.05}$ and $^{+}As^{+}A_{0.10}$ mice compared to $^{+}As^{-}A$ mice (Fig. 4E–G). Significantly lower relative expression of *Cingulin* (0.38 ± 0.14 and 0.63 ± 0.09 vs. 1.04 ± 0.35), *Fodrin* (0.88 ± 0.38 and 0.52 ± 0.06 vs. 1.11 ± 0.31), and *ZO-1* (0.63 ± 0.22 and 0.55 ± 0.29 vs. 1.11 ± 0.13) was also observed in the ileum of $^{-}As^{+}A_{0.05}$ and $^{-}As^{+}A_{0.10}$ mice than $^{-}As^{-}A$ mice (Fig. S3). Previous studies have shown a similar decrease in intestinal tight junctions with alcohol consumption, weakening intestinal barrier function, and allowing epithelial penetration of luminal bacteria and/or bacterial-derived lipopolysaccharides to the blood, causing alcoholic liver disease [48–50].

To reveal mechanisms underlying damaged intestinal tight junctions with alcohol, the levels of MLCK and PTP1B in the ileum were measured. The levels of PTP1B (a phosphatase with a predominant role of

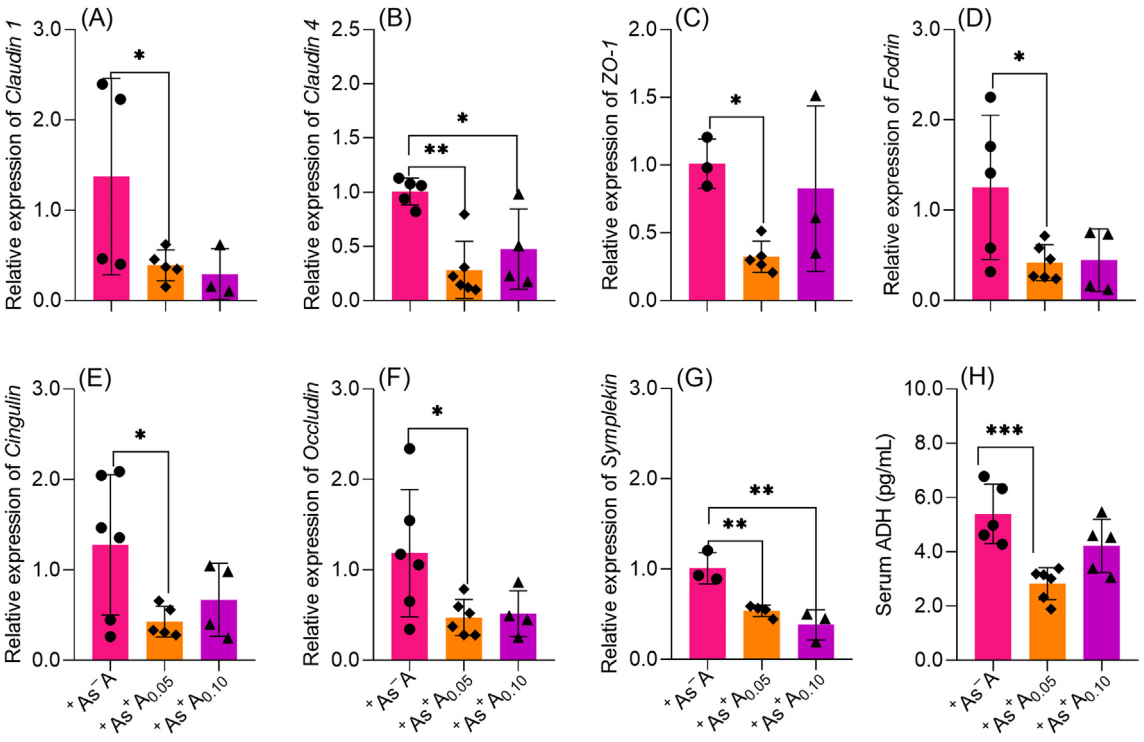

Fig. 5. Comparison of the relative expression of genes encoding for renal glomerular tight junctions (TJs) including *Claudin 1* (**A**), *Claudin 4* (**B**), *Zona-Occludins 1* (*ZO-1*, **C**), *Fodrin* (**D**), *Cingulin* (**E**), *Occludin* (**F**), and *Symplekin* (**G**), and the serum concentration of antidiuretic hormone (ADH, **H**) between mice fed with diets amended with As (6 μg As/g) without and with alcohol co-exposure.

dephosphorylation) in the ileum of $^{+}As^{+}A_{0.05}$ and $^{+}As^{+}A_{0.10}$ mice (0.59 ± 0.16 and 0.54 ± 0.09 ng/g) were significantly ($p < 0.01$) lower than that (0.81 ± 0.13 ng/g) of $^{+}As^{-}A$ mice (Fig. 4H), while the levels of MLCK (a kinase with a dominant role of light chain phosphorylation) were consistent between $^{+}As^{+}A_{0.05}$ and $^{+}As^{+}A_{0.10}$ mice with $^{+}As^{-}A$ mice (Fig. 4I). These results suggested that the liquor-induced damage of paracellular tight junctions was mainly due to the inhibition of intercellular PTP1B in the intestine instead of alcohol's direct role of MLCK activation. Inhibited PTP1B activities can result in increased tyrosine phosphorylation of β-catenin and E-cadherin, which can lead to a loss of the intercellular junctional complexes between E-cadherin and β-catenin and a loss of the homophilic interaction between extracellular domains of E-cadherin, eventually leading to damaged paracellular tight junctions and increased intestinal paracellular permeability [33]. With damaged tight junctions, intestinal permeability to As may be enhanced, thus contributing to higher As bioavailability in alcohol-treated mice (Fig. 1C).

Commonly, higher As bioavailability leads to higher As accumulation in tissue such as liver and kidney [17]; however, this was not the case for liquor-treated mice (Fig. 1F–H), suggesting a unique role of alcohol consumption in the pulling out of As from the body to urine. One probable contributor may be the alcohol-induced damage to glomerular tight junctions, increasing the permeability of the glomerular capillary wall and leading to elevated transglomerular passage of solutes such as As in the glomerular capillaries to urine. In this study, expression of genes encoding for renal tight junctions including *Claudin 1* (0.39 ± 0.17 and 0.29 ± 0.28 vs. 1.37 ± 1.08), *Claudin 4* (0.28 ± 0.26 and 0.47 ± 0.37 vs. 1.00 ± 0.12), *ZO-1* (0.32 ± 0.11 and 0.83 ± 0.61 vs. 1.01 ± 0.18), *Fodrin* (0.42 ± 0.20 and 0.44 ± 0.35 vs. 1.25 ± 0.80), *Cingulin* (0.43 ± 0.17 and 0.67 ± 0.41 vs. 1.28 ± 0.78), *Occludin* (0.47 ± 0.20 and 0.52 ± 0.25 vs. 1.18 ± 0.70), and *Symplekin* (0.54 ± 0.06 and 0.38 ± 0.17 vs. 1.01 ± 0.17) were significantly ($p < 0.05$) lower in $^{+}As^{+}A_{0.05}$ and $^{+}As^{+}A_{0.10}$ mice than $^{+}As^{-}A$ mice (Fig. 5A–G). The studies showed that the tight junction of glomerular parietal epithelial cells is made of *Claudin 1*, *Occludin*, and *ZO-1* [51,52]. The observed decrease in expression of *Claudin 1*, *Occludin*, and *ZO-1* suggested an increase in the permeability of the glomerulus. Glomerulus plays an important role in the production of urine and the excretion of harmful metabolites via glomerular filtration. The glomerular filtration is controlled by the glomerular barrier, which consists of three components: glomerular endothelium, glomerular basement membrane, and glomerular epithelium (podocytes) with slit diaphragm [53]. The studies have shown that disruption of endothelial adherens junctions can induce gaps between endothelial cells and increase endothelial permeability, causing a leaky glomerular "barrier" [54]. With increased endothelial permeability, As in the glomerular capillary may be more readily filtered across the glomerular barrier, thus facilitating As excretion from the body to urine.

Another likely contributor to reduced As retention in the body of liquor-treated mice may be the diuretic function of alcohol [36,37]. In this study, serum concentrations of the ADH were significantly ($p < 0.05$) lower in the $^{+}As^{+}A_{0.05}$ mice than $^{+}As^{-}A$ mice (2.83 ± 0.59 vs. 5.40 ± 1.10 pg/mL) (Fig. 5H). ADH is a hormone that regulates the re-absorption of free water in the collecting tubule by increasing the permeability of the luminal membranes of the principal cells of the collecting ducts of the kidney [55–57]. In the kidney, ADH acts through V2 vasopressin receptors, which cause the aquaporin 2 channel to fuse with the luminal membrane via protein kinase activation, eventually leading to re-absorption of water via aquaporin 2 and concentrating the urine [55–57]. In this study, reduced serum ADH levels in liquor-treated mice indicated that the re-absorption of water was likely reduced when primary urine passed through the tubule, leading to more urine being excreted. As a side-effect of this process, a higher amount of As can be eliminated from the body via urine excretion, thereby contributing to lower As retention in tissue such as liver and kidney. The decreased serum ADH may be one of the body's defense mechanisms to overcome the stress and toxicity of alcohol, aiming to enhance urine production and excretion to rapidly excrete absorbed alcohol via urine.

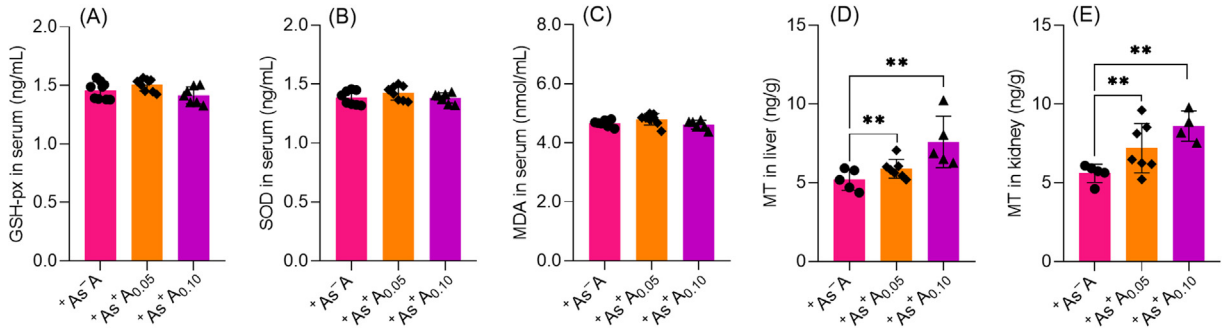

Fig. 6. Effect of alcohol consumption on serum glutathione peroxidase (GSH-px, **A**) and superoxide dismutase (SOD, **B**) activities, serum malondialdehyde (MDA, **C**) level, metallothionine (MT) concentrations in liver (**D**) and kidney (**E**) in mice fed with diets amended with 6 μg As/g.

3.6. As toxicity

Although As bioavailability was enhanced following liquor co-exposure, As toxicity was not higher. Serum GSH (1.50 ± 0.05 and 1.42 ± 0.07 vs. 1.46 ± 0.07 ng/mL), SOD (1.43 ± 0.06 and 1.38 ± 0.04 vs. 1.38 ± 0.06 ng/mL), and MDA (4.80 ± 0.19 and 4.62 ± 0.15 vs. 4.66 ± 0.11 nmol/mL) levels were comparable among $^{+}As^{+}A_{0.05}$, $^{+}As^{+}A_{0.10}$, and $^{+}As^{-}A$ mice (Fig. 6A–C). One reason may be the lower As accumulation in tissue in liquor-treated mice, which may counteract the possible toxicity increase from higher As bioavailability and liquor intake. Another reason may be the significantly ($p < 0.05$) higher MT concentration in the liver (5.88 ± 0.60 and 7.58 ± 1.63 vs. 5.19 ± 0.67 ng/g) and kidney (7.20 ± 1.56 and 8.60 ± 0.96 vs. 5.60 ± 0.58 ng/g) of $^{+}As^{+}A_{0.05}$ and $^{+}As^{+}A_{0.10}$ mice compared to $^{+}As^{-}A$ mice (Fig. 6D and E). Higher tissue MT expression with alcohol exposure has been reported [58,59], which may be a defense mechanism to cope with alcohol stress. MT exhibits a strong As-binding capacity and detoxification function, likely contributing to the lack of increased toxicity with As-liquor co-exposure.

3.7. Environmental implication

Using a mouse bioassay, increased intestinal permeability, increased glomerular filtration, and reduced serum ADH were observed following liquor consumption, which contributed to enhanced As oral bioavailability but lower As accumulation in tissue. These results suggest that although liquor consumption may increase As oral bioavailability to humans, it may also facilitate the elimination of As from the body via urine, thereby reducing As accumulation in tissue and not inducing additional oxidative stress and damage. Alcohol drinking may also have significant impacts on bioavailability and accumulation of other co-contaminants that may be present with As, such as cadmium and lead. Synergistic and/or antagonistic effects on metal(loid) uptake in the presence and absence of alcohol co-exposure warrant further studies. Since human alcohol consumption often shows sex- and age-dependent differences, it is also worth investigating the different responses of females and males and young and old consumers to alcohol consumption. The limitation of the current study is that only a mouse bioassay was employed. To demonstrate the effects of alcohol consumption on As exposure in alcohol drinkers, epidemiological studies investigating variation in urinal As levels between non-alcoholic and alcohol drinkers are warranted.

Author contributions

H.Y.W.: data curation, investigation, roles/Writing-original draft, visualization. A.L.J.: formal analysis, validation, writing-review and editing, supervision. Y.S.Z,: software, investigation. L.Z.Z.: resources, project administration. L.Q.M.: resources, supervision, writing-review and editing. D.M.Z.: resources, supervision, writing-review and editing. H.B.L.: writing-review and editing, conceptualization, methodology, funding acquisition.

Declaration of competing interest

The authors declare the following financial interests/personal relationships which may be considered as potential competing interests:

Hongbo Li reports financial support was provided by National Natural Science Foundation of China and Jiangsu Agricultural Independent Innovation Program.

Acknowledgments

This work was supported by the National Natural Science Foundation of China (42022058, and 41877356), Jiangsu Agricultural Independent Innovation Program [CX(21)3095]. The authors appreciate comments from Dr. Yong-Guan Zhu, Institute of Urban Environment, Chinese Academy of Sciences on the design of the study.

Appendix A. Supplementary data

Supplementary data to this article can be found online at https://doi.org/10.1016/j.eehl.2023.06.003.

References

[1] C. Huang, J. Zhan, Y.J. Liu, D.J. Li, S.Q. Wang, Q.Q. He, Association between alcohol consumption and risk of cardiovascular disease and all-cause mortality in patients with hypertension: a meta-analysis of prospective cohort studies, Mayo Clin. Proc. 89 (9) (2014) 1201–1210.
[2] G. Robert, Moderate alcohol consumption is not associated with reduced all-cause mortality, Am. J. Med. 129 (2) (2016) 180–186.
[3] S. Arranz, G. Chiva-Blanch, P. Valderas-Martínez, A. Medina-Remón, R.M. Lamuela-Raventos, R. Estruch, Wine, beer, alcohol and polyphenols on cardiovascular disease and cancer, Nutrients 4 (7) (2012) 759–781.
[4] I.Y. Millwood, R.G. Walters, X.W. Mei, Y. Guo, L. Yang, Z. Bian, D.A. Bennett, Y.P. Chen, et al., Conventional and genetic evidence on alcohol and vascular disease aetiology: a prospective study of 500000 men and women in China, Lancet 393 (10183) (2019) 1831–1842.
[5] J. Rehm, C. Mathers, S. Popova, M. Thavorncharoensap, Y. Teerawattananon, J. Patra, Alcohol and global burden of disease and injury and economic cost attributable to alcohol use and alcohol-use disorders, Lancet 373 (9682) (2009) 2223–2233.
[6] M.G. Griswold, N. Fullman, C. Hawley, N. Arian, S.R. Zimsen, H.D. Tymeson, Alcohol use and burden for 195 countries and territories 1990-2016: a systematic analysis for the global burden of disease study 2016, Lancet 392 (10152) (2018) 1015–1035.
[7] J. Rehm, G.E. Gmel Sr, G. Gmel, O.M. Hasan, S. Imtiaz, S. Popova, The relationship between different dimensions of alcohol use and burden of disease-an up data, Addiction 112 (6) (2016) 968–1001.
[8] D.J. Carlin, M.F. Naujokas, K.D. Bradham, J. Cowden, M. Heacock, H.F. Henry, J.S. Lee, D.J. Thomas, et al., Arsenic and environmental health: state of the science and future research opportunities, Environ. Health Perspect. 124 (7) (2016) 890–899.
[9] S.M. Cohen, L.L. Arnold, J.S. Tsuji, Inorganic arsenic: a nongenotoxic threshold carcinogen, Curr. Opin. Toxicol. 14 (2019) 8–13.
[10] IARC (International Agency for Research on Cancer), Some drinking water disinfectants and contaminants including arsenic, IARC Monogr. Eval. Carcinog. Risks Hum. 84 (2004) 269–477.

[11] K. Jomova, Z. Jenisova, M. Feszterova, S. Baros, J. Liska, D. Hudecova, C.J. Rhodes, M. Valko, Arsenic: toxicity oxidative stress and human disease, J. Appl. Toxicol. 31 (2) (2011) 95–107.
[12] S. Fendorf, H.A. Michael, A. van Geen, Spatial and temporal variations of groundwater arsenic in South and Southeast Asia, Science 328 (5982) (2010) 1123–1127.
[13] L. Rodríguez-Lado, G.F. Sun, M. Berg, Q. Zhang, H.B. Xue, H.M. Zheng, C.A. Johnson, Groundwater arsenic contamination throughout China, Science 341 (6148) (2013) 866–868.
[14] D. Gilbert-Diamond, K.L. Cottingham, J.F. Gruber, T. Punshon, V. Sayarath, A.J. Gandolfi, E.R. Baker, B.P. Jackson, et al., Rice consumption contributes to arsenic exposure in US women, in: Proceedings of the National Academy of Sciences of the United States of America 108, 2011, pp. 20656–20660, 51.
[15] K.D. Bradham, K.G. Scheckel, C.M. Nelson, P.E. Seales, G.E. Lee, M.F. Hughes, B.W. Miller, A. Yeow, et al., Relative bioavailability and bioaccessibility and speciation of arsenic in contaminated soils, Environ. Health Perspect. 119 (11) (2011) 1629–1634.
[16] M.F. Naujokas, B. Anderson, H. Ahsan, H.V. Aposhian, J.H. Graziano, C. Tompson, W.A. Suk, The broad scope of health effects from chronic arsenic exposure: update on a worldwide public health problem, Environ. Health Perspect. 121 (3) (2013) 295–302.
[17] H.B. Li, M.Y. Li, D. Zhao, J. Li, S.W. Li, A.L. Juhasz, N.T. Basta, Y.M. Luo, et al., Oral bioavailability of as Pb and Cd in contaminated soils dust and foods based on animal bioassays: a review, Environ. Sci. Technol. 53 (18) (2019) 10545–10559.
[18] S.C. Wang, C. Yuan, Y.C. Chen, S.J. Chen, C.H. Lee, C.M. Cheng, Alcohol addiction gut microbiota and alcoholism treatment: a review, Int. J. Mol. Sci. 21 (7) (2020) 6413.
[19] S. Leclercq, S. Matamoros, P.D. Cani, A.M. Neyrinck, F. Jamar, P. Stärkel, K. Windey, V. Tremaroli, et al., Intestinal permeability gut-bacterial dysbiosis and behavioral markers of alcohol-dependence severity, in: Proceedings of the National Academy of Sciences of the United States of America 111, 2014, pp. E4485–E4493, 42.
[20] I.A. Kirpich, N.V. Solovieva, S.N. Leikhter, N.A. Shidakova, O.V. Lebedeva, P.I. Sidorov, T.A. Bazhukova, A.G. Soloviev, et al., Probiotics restore bowel flora and improve liver enzymes in human alcohol-induced liver injury: a pilot study, Alcohol 42 (8) (2008) 675–682.
[21] M.Y. Li, X.Q. Chen, J.Y. Wang, H.T. Wang, X.M. Xue, J. Ding, A.L. Juhasz, Y.G. Zhu, et al., Antibiotic exposure decreases soil arsenic oral bioavailability in mice by disrupting ileal microbiota and metabolic profile, Environ. Int. 151 (2021) 106444.
[22] H.Y. Wang, S. Chen, R.Y. Xue, X.Y. Lin, J.L. Yang, Y.S. Zhang, S.W. Li, A.L. Juhasz, et al., Arsenic ingested early in life is more readily absorbed: mechanistic insights from gut microbiota gut metabolites and intestinal morphology and functions, Environ. Sci. Technol. 57 (2) (2023) 1017–1027.
[23] N.Y. Yin, Z.N. Zhang, X.L. Cai, H.L. Du, G.X. Sun, Y.S. Cui, In vitro method to assess soil arsenic metabolism by human gut microbiota: arsenic speciation and distribution, Environ. Sci. Technol. 49 (17) (2015) 10675–10681.
[24] S.S.C.D.C. Rubin, P. Alava, I. Zekker, G.D. Laing, T. Van de Wiele, Arsenic thiolation and the role of sulfate-reducing bacteria from the human intestinal tract, Environ. Health Perspect. 122 (8) (2014) 817–822.
[25] A.L. Juhasz, E. Smith, J. Weber, M. Rees, A. Rofe, T. Kuchel, R. Naidu, In vivo assessment of arsenic bioavailability in rice and its significance for human health risk assessment, Environ. Health Perspect. 114 (12) (2006) 1826–1831.
[26] H.B. Li, J. Li, D. Zhao, C. Li, X.J. Wang, H.J. Sun, A.L. Juhasz, L.Q. Ma, Arsenic relative bioavailability in rice using a mouse arsenic urinary excretion bioassay and its application to assess human health risk, Environ. Sci. Technol. 51 (8) (2017) 4689–4696.
[27] Y. Sabbagh, H. Giral, Y. Caldas, M. Levi, S.C. Schiavi, Intestinal phosphate transport, Adv. Chron. Kidney Dis. 18 (2) (2011) 85–90.
[28] P.R. Kiela, F.K. Ghishan, Chapter 59: molecular mechanisms of intestinal transport of calcium phosphate and magnesium, in: H.M. Said (Ed.), Physiology of the Gastrointestinal Tract, sixth ed.th ed., Academic Press, Cambridge, Ma, 2018, pp. 1405–1449.
[29] T.Y. Ma, P. Nighot, R. Al-Sadi, Chapter 25: tight junctions and the intestinal barrier, in: H.M. Said (Ed.), Physiology of the Gastrointestinal Tract, sixth ed.th ed., Academic Press, Cambridge, Ma, 2018, pp. 587–639.
[30] I. Hylemon, T. Peters, R. Wise, The leaky gut of alcoholism: possible route of entry for toxic compounds, Lancet 323 (8370) (1984) 179–182.
[31] X.H. Tang, M. Melis, K. Mai, L.J. Gudas, S.E. Trasino, Fenretinide improves intestinal barrier function and mitigates alcohol liver disease, Front. Pharmacol. 12 (2021) 630557.
[32] X. Chi, C.Q. Pan, S.N. Liu, D.Y. Cheng, Z.W. Cao, H.C. Xing, Regulating intestinal microbiota in the prevention and treatment of alcohol-related liver disease, Chin. J. Gastroenterol. Hepatol. 2020 (2020) 6629196.
[33] R. Rao, Endotoxemia and gut barrier dysfunction in alcoholic liver disease, Hepatology 50 (2) (2009) 638–644.
[34] C.R. Weber, D.R. Raleigh, L.P. Su, L. Shen, E.A. Sullivan, Y.M. Wang, J.R. Turner, Epithelial myosin light chain kinase activation induces mucosal interleukin-13 expression to alter tight junction ion selectivity, J. Biol. Chem. 285 (16) (2010) 12037–12046.
[35] W.Q. He, J. Wang, J.Y. Sheng, J.M. Zha, W.V. Graham, J.R. Turner, Contributions of myosin light chain kinase to regulation of epithelial paracellular permeability and mucosal homeostasis, Int. J. Mol. Sci. 21 (3) (2020) 993.
[36] I. Kiyotoshi, O. Kentaro, H. Suzuro, K. Ayu, U. Izumi, Thirst sensation and oral dryness following alcohol intake, Jpn. Den. Sci. Rev. 53 (3) (2017) 78–85.
[37] U.S. Alwis, R. Haddad, T.F. Monaghan, P. Abrams, R. Dmochowski, W. Bower, A.J. Wein, S. Roggeman, et al., Impact of food and drinks on urine production: a systematic review, Int. J. Clin. Pract. 74 (9) (2020) e13539.
[38] J.E. Lee, J.S. Ha, H.Y. Park, E. Lee, Alteration of gut microbiota composition by short-term low-dose alcohol intake is restored by fermented rice liquor in mice, Food Res. Int. 128 (2020) 108800.
[39] A.A. Meharg, G. Norton, C. Deacon, P. Williams, E.E. Adomako, A. Price, Y.G. Zhu, G. Li, et al., Variation in rice cadmium related to human exposure, Environ. Sci. Technol. 47 (11) (2013) 5613–5618.
[40] K. Lu, R.P. Abo, K.A. Schlieper, M.E. Graffam, S. Levine, J.S. Wishnok, J.A. Swenberg, S.R. Tannenbaum, et al., Arsenic exposure perturbs the gut microbiome and its metabolic profile in mice: an integrated metagenomics and metabolomics analysis, Environ. Health Perspect. 122 (3) (2014) 284–291.
[41] M. Coryell, M. McAlpine, N.V. Pinkham, T.R. McDermott, S.T. Walk, The gut microbiome is required for full protection against acute arsenic toxicity in mouse models, Nat. Commun. 9 (2018) 5424.
[42] K.J. Livak, T.D. Schmittgen, Analysis of relative gene expression data using real-time quantitative PCR and the 2(-delta delta C(T)) method, Methods 25 (4) (2001) 402–408.
[43] A. Vassallo, A. Mirijello, A. Ferrulli, M. Antonelli, R. Landolfi, A. Gasbarrini, G. Addolorato, Review article: alcohol and gut microbiota-the possible role of gut microbiota modulation in the treatment of alcoholic liver disease, Aliment. Pharmacol. Ther. 41 (10) (2015) 917–927.
[44] M. Calatayud, C. Xiong, G.D. Liang, G. Raber, K. Francesconi, T. Van de Wiele, Salivary and gut microbiomes play a significant role in in vitro oral bioaccessibility, biotransformation, and intestinal absorption of arsenic from food, Environ. Sci. Technol. 52 (24) (2018) 14422–14435.
[45] S.K. Sarin, A. Pande, B. Schnabl, Microbiome as a therapeutic target in alcohol-related liver disease, J. Hepatol. 70 (2) (2019) 260–272.
[46] D.J. Thompson, A chemical hypothesis for arsenic methylation in mammals, Chem. Biol. Interact. 88 (2–3) (1993) 89–114.
[47] K.T. Kitchin, Recent advances in arsenic carcinogenesis: modes of action animal model systems and methylated arsenic metabolites, Toxicol. Appl. Pharmacol. 172 (3) (2001) 249–261.
[48] A. Parlesak, C. Schafer, T. Schutz, J.C. Bode, C. Bode, Increased intestinal permeability to macromolecules and endotoxemia in patients with chronic alcohol abuse in different stages of alcohol-induced liver disease, J. Hepatol. 32 (5) (2002) 742–747.
[49] R.K. Rao, A. Seth, P. Sheth, Recent advances in alcoholic liver disease Irole of intestinal permeability and endotoxemia in alcoholic liver disease, Am. J. Physiol. Gastrointest. Liver Physiol. 286 (6) (2004) G881–G884.
[50] V. Purohit, J.C. Bode, C. Bode, D.A. Brenner, M.A. Choudhry, F. Hamilton, Alcohol intestinal bacterial growth intestinal permeability to endotoxin and medical consequences: summary of a symposium, Alcohol 42 (5) (2008) 349–361.
[51] J.H. Hou, The kidney tight junction (Review), Int. J. Mol. Med. 34 (2014) 1451–1457.
[52] T. Ohse, A.M. Chang, J.W. Pippin, G. Jarad, K.L. Hudkins, C.E. Alpers, J.H. Miner, S.J. Shankland, A new function for parietal epithelial cells: a second glomerular barrier, Am. J. Physiol. Ren. Physiol. 297 (2009) F1566–F1574.
[53] M. Camici, Renal glomerular permselectivity and vascular endothelium, Biomed, Pharm. Times 59 (2005) 30–37.
[54] M. Corada, M. Mariotti, G. Thurston, K. Smith, R. Kunkel, M. Brockhaus, et al., Vascular endothelial-cadherin is an important determinant of microvascular integrity in vivo, Proc. Natl. Acad. Sci. USA 96 (1999) 9815–9820.
[55] P.C.A. Kam, S. Williams, F.F.Y. Yoong, Vasopressin and terlipressin: pharmacology and its clinical relevance, Anaesthesia 59 (2004) 993–1001.
[56] E. Poch, A. Molina, G. Pîñeiro, Syndrome of inappropriate antidiuretic hormone secretion, Med. Clínica 159 (2022) 139–146.
[57] S.A. Rivkees, Differentiating appropriate antidiuretic hormone secretion, inappropriate antidiuretic hormone secretion and cerebral salt wasting: the common, uncommon, and misnamed, Curr. Opin. Pediatr. 20 (2008) 448–452.
[58] K.D. Loney, K.R. Uddin, S.M. Singh, Strain-specific brain metallothionein II (MT-II) gene expression its ethanol responsiveness and association with ethanol preference in mice, Alcohol Clin. Exp. Res. 27 (3) (2003) 388–395.
[59] E. Grasselli, A. Voci, I. Demori, R. De Matteis, A.D. Compalati, G. Gallo, L. Vergani, Effect of binge ethanol on lipid homeostasis and oxidative stress in a rat model of nonalcoholic fatty liver disease, J. Physiol. Biochem. 70 (2014) 341–353.